

Cooperative C—H···O Hydrogen Bonding in CO₂–Lewis Base Complexes: Implications for Solvation in Supercritical CO₂

Poovathinthodiyil Raveendran and Scott L. Wallen*

Contribution from the Department of Chemistry, CB# 3290, Kenan and Venable Laboratories, The University of North Carolina, Chapel Hill, North Carolina 27599-3290

Received November 3, 2001

Abstract: Understanding the fundamental principles for the design of CO₂-philic materials is of growing importance due to the potential for enabling “green” chemistry and technologies in liquid and supercritical CO₂ as alternative solvent systems. Recently, there have been numerous efforts to develop hydrocarbon-based CO₂-philes containing carbonyl groups, which are known to interact through a Lewis acid–Lewis base (LA–LB) interaction with CO₂ molecules, thereby providing the necessary solvation energy for dissolution. In this work, we investigate the role of a weaker, but cooperative, C–H···O hydrogen bond as an additional stabilizing interaction in the solvation of polycarbonyl moieties with hydrogen atoms attached directly to the carbonyl carbon or to the α -carbon atom. Ab initio calculations are performed on simple intermolecular complexes of CO₂ with compounds capable of acting as Lewis bases. Systems studied in different interaction configurations include formaldehyde, acetaldehyde, acetic acid, and methyl acetate, as model carbonyl compounds, and dimethyl sulfoxide as a model system for the sulfonyl group. Interaction energies, vibrational frequencies, charge transfer, and other molecular properties are calculated. Results indicate that C–H···O hydrogen bonds may be an important stabilizing interaction that merits consideration in the design of future CO₂-philes.

1. Introduction

Miscibility and dissolution of materials in liquid and supercritical CO₂ (scCO₂) have gained considerable attention in the recent past due to the advantages of CO₂ over conventional organic solvents and the many potential applications in “green” chemistry.^{1–10} CO₂ is regarded as an environmentally benign solvent because of its nontoxicity, but more importantly, it is an excellent choice as a solvent due to the ease of solvent removal, its abundance, low cost, and tunability of solvent parameters.⁴ The low solubility of the majority of polar and ionic materials has, however, been a serious limitation in expanding the possibilities of this solvent system. Thus, the fundamental principles for the design of CO₂-philic molecules including amphiphiles have attracted great interest, and different molecular level approaches have been used to “CO₂-philize”

compounds that are otherwise insoluble in CO₂.^{1,5,6,10} The first, and thus far the most widely, applied method is the introduction of fluorocarbons.¹⁰ Though the interaction between CO₂ and fluorocarbons is very weak,^{11–12} fluorocarbons exhibit high solubility in liquid and scCO₂. Conflicting theories on the nature of this interaction have been put forth, and the debate is still active.^{10–13}

Fluorocarbon-based CO₂-philes are expensive; thus, there is current interest in the development of inexpensive, hydrocarbon-based CO₂-philes. The specific interaction of CO₂ molecules with Lewis base groups, especially carbonyl groups,^{14–16} has also been utilized in the design of CO₂-philic materials.^{6–7} Beckman and co-workers synthesized hydrocarbon-based, carbonyl-supported, poly(ether-carbonate) copolymers soluble in liquid CO₂ by maximizing the entropic and enthalpic contributions to solvation.⁶ The investigators also reported a high solubility for poly(propylene glycol)acetate with 21 repeat units.⁶ This necessitates a close examination of the nature of the interaction of CO₂ with various functional groups containing carbonyl moieties (such as acetate groups). Several experimental

* To whom correspondence should be addressed. E-mail: wallen@email.unc.edu.

- (1) DeSimone, J. M.; Guan, Z.; Elsbernd, C. S. *Science* **1992**, *267*, 945–947.
- (2) Wells, S. L.; DeSimone, J. M. *Angew. Chem., Int. Ed.* **2001**, *40*, 518–527.
- (3) Eckert, C. A.; Knuston, B. L.; Debendetti, P. G. *Nature* **1996**, *373*, 313–318.
- (4) McHugh, M. A.; Krukonic, V. J. *Supercritical Fluid Extractions: Principles and Practice*, 2nd ed.; Butterworth-Heinemann: Boston, MA, 1994.
- (5) Rindfleisch, F.; DiNoia, T. P.; McHugh, M. A. *J. Phys. Chem.* **1996**, *100*, 15581–15587.
- (6) Sarbu, T.; Styranec, T.; Beckman, E. J. *Nature* **2000**, *405*, 165–168.
- (7) Sarbu, T.; Styranec, T.; Beckman, E. J. *Ind. Eng. Chem. Res.* **2000**, *39*, 4678–4683.
- (8) Consani, K. A.; Smith, R. D. *J. Supercrit. Fluids* **1990**, *3*, 51–65.
- (9) Johnston, K. P.; Harrison, K. L.; Clarke, M. J.; Howdle, S. M.; Heitz, M. P.; Bright, F. V.; Carrier, C.; Randolph, T. W. *Science* **1996**, *271*, 624–626.
- (10) Laintz, K. E.; Wai, C. M.; Yonker, C. R.; Smith, R. D. *J. Supercrit. Fluids* **1991**, *4*, 194–198.

- (11) Yee, G. G.; Fulton, J. L.; Smith, R. D. *J. Phys. Chem.* **1996**, *96*, 6172–6182.
- (12) Diep, P.; Jordan, K. D.; Johnson, J. K.; Beckman, E. J. *J. Phys. Chem. A* **1998**, *102*, 2231–2236.
- (13) (a) Dardin A.; DeSimone J. M.; Samulski E. T. *J. Phys. Chem. B* **1998**, *102*, 1775–1780. (b) Yonker, C. R.; Palmer, B. J. *J. Phys. Chem. A* **2001**, *105*, 308–314.
- (14) Nelson, M. R.; Borkman, R. F. *J. Phys. Chem. A* **1998**, *102*, 7860–7863.
- (15) Kazarian, S. G.; Vincent, M. F.; Bright, F. V.; Liotta, C. L.; Eckert, C. A. *J. Am. Chem. Soc.* **1996**, *118*, 1729–1736.
- (16) Meredith, J. C.; Johnston, K. P.; Seminario, J. M.; Kazarian, S. G.; Eckert, C. A. *J. Phys. Chem.* **1996**, *100*, 10837–10848.

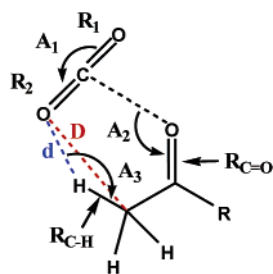


Figure 1. Typical interaction geometry of CO₂ complexes involving a cooperative C–H···O hydrogen bond associated with a typical LA–LB interaction between CO₂ and a Lewis base system (e.g., a carbonyl functionality) as in the interaction between CO₂ and an acetate group. *D* and *d* represent the C···O and the H···O distances for the C–H···O interaction, respectively. Angles *A*₁, *A*₂ and *A*₃ are the respective angles O=C=O, >C=O···C, and C–H···O, defining the structure of the complexes. *R*₁ and *R*₂ are bond lengths (C=O) of the “free” and “complexed” bonds of CO₂. *R*_{C=O} and *R*_{C–H} represent the bond lengths of the >C=O group and the C–H bond involved in C–H···O hydrogen bond, respectively.

and theoretical studies have been carried out to estimate the nature and extent of these interactions. Using IR spectroscopy Kazarian et al.^{15,16} studied the specific interaction between CO₂ and carbonyl groups by investigating the lifting of the degeneracy of the CO₂ bending modes, ν_2 , as a result of these interactions. These researchers speculated that these interactions could be responsible for the swelling of polyacrylates by CO₂. Following these experimental studies, Nelson and Borkman used ab initio calculations¹⁴ to quantify the splitting of the ν_2 mode of CO₂ upon interaction with carbonyl groups in simple molecules. However, after a closer examination of their results and the optimized geometries of the complexes reported,¹⁴ we have identified the probability of another weaker, but significant type of interaction, a C–H···O hydrogen bond.^{17–25} We hypothesize that this interaction acts cooperatively with the CO₂–carbonyl interaction in systems having a hydrogen atom attached to the carbonyl carbon or the α -carbon atom as shown in Figure 1.

In C–H···O hydrogen bonding, the C–H acts as the proton donor, and these interactions are in general rather weak compared to the conventional X–H···Y-type of hydrogen bond. A shortening of the C–H bond and a blue shift of the C–H stretching frequency characterize these interactions, while for typical O–H···O hydrogen bonding, the O–H bonds are stretched as a result of the hydrogen-bond formation.^{26,27} Extensive theoretical and experimental investigations have been carried out in the recent literature to identify the strength and directionality of these relatively weak interactions.^{28–35} Dixon

and co-workers^{28,29} reported computational evidence suggesting that C α –H···O=C< interactions are of sufficient strength to exert a significant influence on protein structure. It was reported that in *N,N*-dimethyl formamide dimers, each of these interactions provides a stabilization energy of at least –2.1 kcal/mol.²⁸ Due to the apparently opposite features of these interactions compared to conventional hydrogen bonds, Hobza and co-workers have even described²⁶ these as “anti-hydrogen bonds”. Scheiner and co-workers³⁰ carried out detailed ab initio molecular orbital calculations to probe the fundamental nature of the C–H···O hydrogen bond and compared this to the O–H···O hydrogen bond. They observed that, although C–H···O bonds are weaker than O–H···O bonds, their binding energy dies off more gradually as the distance between the two subunits is increased.³⁰

It is widely accepted that C–H···O hydrogen bonds play an important role in determining macromolecular conformation,³⁴ crystal packing,^{19,21–25} molecular recognition processes,³⁵ stabilization of inclusion complexes,³⁶ and the activity³⁷ of biological macromolecules. High-resolution crystal structures of proteins have recently revealed close C–H···O contacts, suggesting a biological role for these weak interactions in determining the conformation of these molecules. The majority of the reported C–H···O contacts in proteins involve hydrogen atoms attached to the α -carbons in the peptide backbone, as these C–H bonds are relatively more polarized due to the electron withdrawal by the C=O and N–H groups. In crystal engineering, these weak interactions play a crucial role in directing the three-dimensional growth of crystals. Even in small molecules, C–H···O hydrogen bonding can play an important role in cluster formation, condensation and related phenomena. For example it has been reported³⁸ that in dimethyl ether-terminated methanol clusters, the C–H···O interactions guide the formation of cyclic tetramer structures rather than the expected chain structures. These examples indicate that these relatively weak interactions are ubiquitous and play an important role in molecular structure.

In the present work we investigate the role of cooperative C–H···O hydrogen bonds as a CO₂-philic stabilization factor in addition to the LA–LB interactions between CO₂ and the carbonyl group by using ab initio calculations. For this purpose,

- (17) Sutor, D. J. *Nature* **1962**, *193*, 68–69.
 (18) Green, R. D. *Hydrogen Bonding by C–H Groups*; Wiley-Interscience: New York, 1974.
 (19) Desiraju, G. R.; Steiner, T. *The Weak Hydrogen Bond in Structural Chemistry and Biology*; Oxford University Press: Oxford, 1999.
 (20) Scheiner, S. *Hydrogen Bonding: A Theoretical Perspective*; Oxford University Press: Oxford, 1997.
 (21) Steiner, T. *Crystallogr. Rev.* **1996**, *6*, 1–57.
 (22) Steiner, T. *Chem. Commun.* **1997**, 727–734.
 (23) (a) Desiraju, G. R. *Acc. Chem. Res.* **1996**, *29*, 441–449. (b) Hobza, P.; Havlas, Z. *Chem. Rev.* **2000**, *100*, 4253–64.
 (24) Pedireddi, V. R.; Chatterjee, S.; Ranganathan, A.; Rao, C. N. R. *J. Am. Chem. Soc.* **1997**, *119*, 10867–10868.
 (25) Wahl, M. C.; Rao, S. T.; Sundaralingam, M. *Nat. Struct. Biol.* **1996**, *3*, 24–31.
 (26) Hobza, P.; Spirko, V.; Havlas, Z.; Buchhold, K.; Reimann, B.; Barth, H.; Brutschy, B. *Chem. Phys. Lett.* **1999**, *299*, 180–186.
 (27) Hobza, P.; Spirko, V.; Selzle, H. L.; Schlag, W. *J. Phys. Chem. A* **1998**, *102*, 2501–2504.

- (28) Vargas, R.; Garza, J.; Dixon, D. A.; Hay, B. P. *J. Am. Chem. Soc.* **2000**, *122*, 4750–4755.
 (29) Dixon, D. A.; Hay, B. P. *J. Phys. Chem. A* **2000**, *104*, 5115–5121.
 (30) Gu, Y.; Kar, T.; Scheiner, S. *J. Am. Chem. Soc.* **1999**, *121*, 9411–9422.
 (31) Jedlovsky, P.; Turi, L. *J. Phys. Chem. B* **1997**, *101*, 5429–5436.
 (32) Chang, H.; Jiang, J.; Lin, S. H.; Weng, N.; Chao, M. *J. Chem. Phys.* **2001**, *115*, 3215–3218.
 (33) Scheiner, S.; Gu, Y.; Kar, T. *J. Mol. Struct. (THEOCHEM)* **2000**, *500*, 441–452.
 (34) Scheiner, S.; Kar, T.; Gu, Y. *J. Biol. Chem.* **2000**, *276*, 9832–9837.
 (35) (a) Shimon, L. J. W.; Vaida, M.; Addadi, L.; Lahav, M.; Leiserowitz, L. *J. Am. Chem. Soc.* **1990**, *112*, 6215–6220. (b) Keegstra, E. M. D.; Spek, A. L.; Zwikker, J. W.; Jenneskens, L. W. *J. Chem. Soc., Chem. Commun.* **1994**, 1633–1634. (c) Desiraju, G. R. *Angew. Chem., Int. Ed. Engl.* **1995**, *34*, 2311–2327.
 (36) (a) Steiner, T.; Saenger, W. *J. Chem. Soc., Chem. Commun.* **1995**, 2087–2088. (b) Braga, D.; Grepioni, F.; Byrne, J. J.; Wolf, A. *J. Chem. Soc., Chem. Commun.* **1995**, 125–126. (c) Behrens, P.; van de Goor, G.; Freyhardt, C. C. *Angew. Chem., Int. Ed. Engl.* **1996**, *34*, 2680–2682. (d) Houk, K. N.; Menzer, S.; Newton, S. P.; Raymo, R. M.; Stoddart, J. F.; Williams, D. J. *J. Am. Chem. Soc.* **1999**, *121*, 1479–1487.
 (37) (a) Egli, M.; Gessner, R. V. *Proc. Natl. Acad. Sci. U.S.A.* **1995**, *92*, 180–184. (b) Leonard, G. A.; McAuly-Hecht, K.; Brown, T.; Hunter, W. N. *Acta Crystallogr., Sect. D* **1995**, *51*, 136–139. (c) Berger, I.; Egli, M.; Rich, A. *Proc. Natl. Acad. Sci. U.S.A.* **1996**, *93*, 12116–12121. (d) Musah, R. A.; Jensen, G. M.; Rosenfeld, R. J.; McRee, D. E.; Goodin, D. B. *J. Am. Chem. Soc.* **1997**, *119*, 9083–9084.
 (38) Raveendran, P.; Zimmermann, D.; Häber, T.; Suhm, M. A. *Phys. Chem. Chem. Phys.* **2000**, *2*, 3555–3563.

we have chosen to study the interaction of some of the simplest carbonyl compounds with CO₂, namely, formaldehyde (HCHO), acetaldehyde (AcH), methyl acetate (MeOAc), and acetic acid (AcOH). Similar interactions are investigated in the case of another Lewis base functionality (sulfonyl) in dimethyl sulfoxide (DMSO).

2. Computational Methods

Ab initio calculations were performed using the Gaussian98 program.³⁹ Preliminary geometry optimizations were carried out at the Hartree–Fock (HF) level using 3-21G and 6-31G, as well as density functional theory (DFT). More exact calculations of geometry, energies, and vibrational frequencies were performed at the second-order Møller–Plesset (MP2)⁴⁰ level to include the effects of electron correlation. For MP2 level optimizations, we employed the 6-31+G* basis set, and all the optimizations were carried out using the Berny optimization procedure in Gaussian98. The energies at these optimized geometries (single-point) were calculated using Dunning’s polarized correlation-consistent aug-cc-pVDZ basis set, augmented by diffuse functions.⁴¹ Thus, throughout this paper, while referring to the single-point energies at MP2/aug-cc-pVDZ level for the geometries optimized at MP2/6-31+G* level, we simply refer to them as MP2/aug-cc-pVDZ energies. Interaction energies (ΔE) of these complexes for different interaction geometries were calculated using the “supermolecule” method,⁴² as the difference in energy between each complex and the sum of the isolated monomers according to:

$$\Delta E = E_{AB} - (E_A + E_B) \quad (1)$$

where E_{AB} is the energy of the optimized complex (AB) and E_A and E_B are the respective energies of the optimized monomers A and B. The basis set superposition errors (BSSE) were calculated using the counter-poise method of Boys and Bernardi.⁴³ Vibrational frequencies are calculated at the MP2/6-31+G* level. While some previous studies show that DFT calculations using the B3LYP functional yield results comparable to those at the MP2 level, recent experimental results reveal that DFT at this level may not be accurate for calculating changes in vibrational frequencies as a result of complexation.³⁸ Thus, we restrict our discussions to the MP2 level binding energies of the optimized geometries. Molden was used to visualize the results of the Gaussian98 calculations.⁴⁴

3. Results and Discussion

Solvation in scCO₂ has been of great theoretical as well as experimental interest.⁴⁵ It is clear that solvation in CO₂ depends not only on the interactions between CO₂ and the CO₂-philic functional group but also on their relative strength in comparison with the solvent–solvent interactions⁴⁶ and the solute–solute

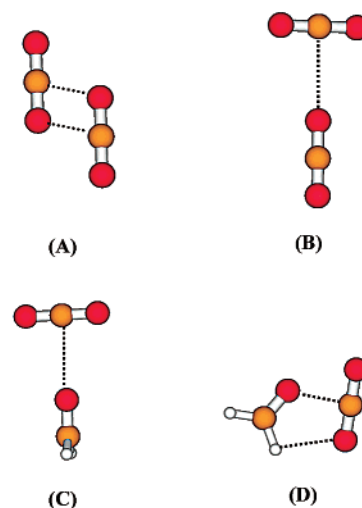


Figure 2. Optimized structures (MP2/6-31+G*) for (A) the “slipped” parallel geometry (C_{2h} symmetry) and (B) the T-geometry (C_{2v} symmetry) of the CO₂ dimer as well as (C) the T-structure (C_{2v} symmetry) and (D) the proton side (C_s symmetry) configuration for the HCHO–CO₂ complex.

interactions. The structure and binding of CO₂ dimer^{46–49} and trimer^{48,49} have been extensively studied using high-level ab initio calculations as well as high-resolution spectroscopy. It is well established that for the CO₂ dimer, there are two favored configurations—the slipped parallel (C_{2h} symmetry) as well as the T-shaped (C_{2v} symmetry) geometries. Both the theoretical and the experimental investigations have shown that among these structures, the slipped parallel geometry is preferred over the T-shaped geometry in the dimers observed in gas phase. It was reported⁴⁸ that the interaction energies of the slipped parallel and T-geometries are -1.33 and -1.11 kcal/mol, respectively, at the MP2/aug-cc-pVQZ level. The interaction energies calculated⁴⁸ using the MP2-R12 method with the *13s8p6d5f* basis set for these two geometries were -1.48 kcal/mol and -1.18 kcal/mol, respectively. Spectroscopic studies by Miller and co-workers⁴⁷ have shown that the C_{2h} geometry is favored over the C_{2v} geometry in low-temperature molecular clusters. Since energies of the various solute–solvent complexes presented in this work are at the MP2/aug-cc-pVDZ level (after optimizations at the MP2/6-31+G* level), we have employed the same level of theory for the calculation of the CO₂ dimer structures also, for comparison purposes. The optimized geometries are shown in Figure 2A and B, respectively. The BSSE corrected interaction energies (ΔE^c) are -1.1 kcal/mol and -0.94 kcal/mol for the C_{2h} and the C_{2v} geometries, respectively (see Table 1).

Ab initio calculations⁴⁸ and high-resolution IR spectroscopic studies⁴⁹ reveal that the CO₂ trimer exists predominantly in the ring structure. The preference for the ring structures in small clusters arises from the fact that ring structures maximize the number of possible LA–LB interactions between the CO₂

(39) Frisch, M. J.; Trucks, G. W.; Schlegel, H. B.; Scuseria, G. E.; Robb, M. A.; Cheeseman, J. R.; Zakrzewski, V. G.; Montgomery, J. A., Jr.; Stratmann, R. E.; Burant, J. C.; Dapprich, S.; Millam, J. M.; Daniels, A. D.; Kudin, K. N.; Strain, M. C.; Farkas, O.; Tomasi, J.; Barone, V.; Cossi, M.; Cammi, R.; Mennucci, B.; Pomelli, C.; Adamo, C.; Clifford, S.; Ochterski, J.; Petersson, G. A.; Ayala, P. Y.; Cui, Q.; Morokuma, K.; Malick, D. K.; Rabuck, A. D.; Raghavachari, K.; Foresman, J. B.; Cioslowski, J.; Ortiz, J. V.; Stefanov, B. B.; Liu, G.; Liashenko, A.; Piskorz, P.; Komaromi, I.; Gomperts, R.; Martin, R. L.; Fox, D. J.; Keith, T.; Al-Laham, M. A.; Peng, C. Y.; Nanayakkara, A.; Gonzalez, C.; Challacombe, M.; Gill, P. M. W.; Johnson, B. G.; Chen, W.; Wong, M. W.; Andres, J. L.; Head-Gordon, M.; Replogle, E. S.; Pople, J. A. *Gaussian 98*; Gaussian, Inc.: Pittsburgh, PA, 1998.

(40) (a) Møller, C.; Plesset, M. S. *Phys. Rev.* **1934**, *46*, 618–624. (b) Pople, J. A.; Binkley, J. S.; Seeger, R. *Int. J. Quantum Chem. Symp.* **1976**, *10*, 1–19.

(41) (a) Woon, D. E.; Dunning, T. H. *J. Chem. Phys.* **1993**, *98*, 1358–1371. (b) Dunning, T. H. *J. Phys. Chem. A* **2000**, *104*, 9062–9080.

(42) Morokuma, K.; Kitaura, K. In *Molecular Interactions*; Ratajczak, H., Orville-Thomas, W. J., Eds.; Wiley: New York, 1980; Vol. 1, pp 21–87.

(43) Boys, S. F.; Bernardi, F. *Mol. Phys.* **1970**, *19*, 553–556.

(44) Schaftenaar, G.; Noordik, J. H. *J. Comput.-Aided Mol. Des.* **2000**, *14*, 123–134.

(45) (a) Bukowski, R.; Szalewicz, K.; Chabalowski, C. F. *J. Phys. Chem. A* **1999**, *103*, 7322–7340. (b) Salaniwal, S.; Cui, S.; Cochran, H. D.; Cummings, P. T. *Ind. Eng. Chem. Res.* **2000**, *39*, 4543–4554. (c) Rice, J. K.; Niemeyer, E. D.; Dunbar, R. A.; Bright, F. V. *J. Am. Chem. Soc.* **1995**, *117*, 5830–5839. (d) Ngo, T. T.; Bush, D.; Eckert, C. A.; Liotta, C. L. *AIChE J.* **2001**, *47*, 2566–2572.

(46) (a) Illies, A. J.; McKee, M. L.; Schlegel, H. B. *J. Phys. Chem.* **1987**, *91*, 3489–3494. (b) Nesbitt, D. J. *Chem. Rev.* **1988**, *88*, 843–870.

(47) Jucks, K. W.; Huang, Z. S.; Miller, R. E.; Lafferty, W. J. *J. Chem. Phys.* **1987**, *86*, 4341–4346.

(48) Tszuzuki, S.; Klopper, W.; Lüthi, H. P. *J. Chem. Phys.* **1999**, *111*, 3846–3854.

(49) Weida, M. J.; Nesbit, D. J. *J. Chem. Phys.* **1996**, *105*, 10210–10223.

Table 1. BSSE Corrected Interaction Energies (ΔE^c) for the CO₂ Complexes with HCHO, AcH, MeOAc, AcOH, and DMSO along with Those of the CO₂ Dimer for Different Interaction Configurations, Calculated at the RHF and the MP2 Levels of Theory Using aug-cc-pVDZ Basis Set^a

molecular species	ΔE^c (RHF) (kcal/mol)	ΔE^c (kcal/mol)	ΔE^c (MP2) (kcal/mol)
HCHO–CO ₂ (T)	–1.40	–0.52	–1.92
HCHO–CO ₂ (P)	–1.84	–0.59	–2.43
AcH–CO ₂ (M)	–1.76	–0.72	–2.52
AcH–CO ₂ (P)	–2.08	–0.61	–2.69
MeOAc–CO ₂ (M)	–1.96	–0.86	–2.82
MeOAc–CO ₂ (E)	–1.67	–0.97	–2.64
AcOH–CO ₂ (M)	–2.00	–0.80	–2.80
CO ₂ dimer (II)	–0.29	–0.82	–1.10
CO ₂ dimer (T)	–0.24	–0.70	–0.94
DMSO–CO ₂	–2.15	–1.27	–3.42
H ₂ O–H ₂ O ^b			–4.11 ^b

^a The optimizations were carried out at the MP2/6-31+G* level and single-point energies for the optimized geometries were computed at MP2/aug-cc-pVDZ level. For comparison, the ΔE^c for water dimer is shown. ^bReference 30. ^c ΔE^c is the electron correlation component of ΔE^c (MP2).

molecules, exceeding by one the number found in the chain and branched structures. The ring structures can also enhance the cooperativity. The situation is similar to the growth of the clusters of water,⁵⁰ methanol⁵¹ and *tert*-butanol⁵² where the ring structures dominate in the range $n = 3–5$ and on further increase in n , the topology changes to chains and branched chains since the preference for the ring structure slowly goes away. In fact, the signatures from neutron scattering data and molecular dynamics simulations of liquid CO₂ indicate that the interaction geometries in liquid CO₂ are closer to the T-interaction geometry.⁵³

Although the net dipole moment for CO₂ is zero, CO₂ is not a nonpolar solvent, but a quadrupolar solvent.⁵⁴ There is a clear charge separation in the CO₂ molecule with the bond electron density being polarized more toward the oxygen atoms, leaving the carbon atom with a partial positive charge and the two oxygen atoms with partial negative charges. Thus, the electron-deficient carbon atom can act as a Lewis acid, while the oxygen atoms, though less effectively, can act as Lewis base moieties. The situation is somewhat analogous to the case of H₂O, which can act both as a Lewis acid as well as a Lewis base. However, in CO₂ these interactions are rather weak compared to that in H₂O, considering the unique hydrogen-bond networks in the latter, making CO₂ a much less effective solvent for polar materials. Nevertheless, it has been shown that the LA–LB interactions between CO₂ and carbonyl functional groups are almost half as strong as the interactions between two water molecules.¹⁴ As mentioned previously, IR spectroscopic studies by Kazarian et al. have clearly demonstrated the nondegeneracy of the CO₂ bending modes, ν_2 , when complexed to the carbonyl groups of solid polymers.¹⁵ This specific interaction (LA–LB) has been the focus of the design of CO₂-philic polymers, which have potential for use in variety of green chemistry applications.

However, to maximize the CO₂-philicity, one should investigate what type of functionality should be the most energetically suitable and elucidate the fundamental nature of such solute–solvent interactions governing solvation.

3.1. Energetics and Geometric Considerations. The optimized geometries for the HCHO–CO₂ complex are shown in Figure 2, C (C_{2v}) and D (C_s), respectively. In the C_{2v} geometry (HCHO–CO₂ (T)), the carbonyl carbon, oxygen, and the C-atom of CO₂ are linear, and their interaction is restricted to a simple LA–LB interaction between CO₂ and the carbonyl group. However, it is noteworthy that the CO₂ molecule is oriented perpendicular to the plane of the formaldehyde molecule. The geometry in which CO₂ is in the same plane as formaldehyde is energetically unstable and is readily routed to the out-of-plane geometry. This is important since both the oxygen lone pairs of the carbonyl group are in the plane of the molecule. It is plausible that in this geometry, the interaction between the carbonyl oxygen and the C-atom of CO₂ is more electrostatic in nature, and the out-of plane arrangement of CO₂ minimizes the repulsive interactions between the lone pairs of the carbonyl oxygen and the oxygen atoms of CO₂, especially considering the partial negative charges on these oxygen atoms. Another possibility is the involvement of the carbonyl π -electrons in the interaction. The interaction energy (ΔE^c) corresponding to this geometry is –1.92 kcal/mol (Table 1).

In the C_s geometry (HCHO–CO₂ (P)), however, CO₂ is planar with the formaldehyde molecule, as the carbonyl oxygen interacts with the carbon atom of CO₂ and one of the oxygen atoms of CO₂ points toward one of the aldehyde hydrogen atoms. The geometric parameters for this complex suggest the presence of a weak, cooperative C–H···O interaction as an additional stabilization for this geometry compared to the C_{2v} geometry. The interaction energy corresponding to this geometry is –2.43 kcal/mol. In this configuration, having a five-membered ring including the hydrogen, the carbon, and oxygen atoms of the aldehyde along with the carbon and one of the oxygen atoms of the CO₂ molecule, a weak electron delocalization cannot be ruled out considering the contracting nature of the C–H···O bond. The H···O distance (d) is 2.71 Å, and the C···O distance (D) is 3.24 Å (Figures 1 and 2), well within the reported limits of D to qualify the interaction as a C–H···O hydrogen bond (4.0 Å).^{23a}

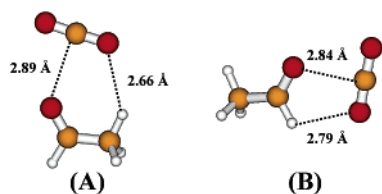
One possible explanation for the higher interaction energy of the C_s geometry is that the oxygen lone pairs are in plane, at 120° with the >C=O bond, and this would be the ideal condition for the interaction between the carbonyl group and the CO₂ molecule (>C=O···C angle, $A_2 = 120^\circ$). However, the >C=O···C angle for the C_s geometry of the HCHO–CO₂ complex is 111.0°, suggesting a deviation from the ideal condition due to or for the involvement of a C–H···O hydrogen bond. From a qualitative view, since the CO₂ oxygen is sp²-hybridized, the preferred C=O···H angle should be 120°. However, this is not a rigid rule since the variation in energy with angular deviation is small.³⁰ The C=O···H (the C=O of CO₂ involved in hydrogen bonding) angle for the C_s geometry of the HCHO–CO₂ complex is 109.5°. In all these interactions, the CO₂ molecule is bent slightly, caused by deviation of the carbon atom from the sp-hybridization. Although HCHO presents the simplest but convincing case for the existence of cooperative C–H···O interactions, it is of interest to investigate

- (50) Xantheas, S. S. *J. Chem. Phys.* **1994**, *100*, 7523–7534.
 (51) (a) Hagemester, F. C.; Gruenloh, C. J.; Zwier, T. S. *J. Phys. Chem. A* **1998**, *102*, 82–94. (b) Häber, T.; Schmitt, U.; Suhm, M. A. *Phys. Chem. Chem. Phys.* **1999**, *1*, 5553–5582. (c) Wallen, S. L.; Palmer, B. J.; Garrett, B. G.; Yonker, C. R. *J. Phys. Chem.* **1996**, *100*, 3959–3964.
 (52) (a) Zimmerman, D.; Häber, T.; Schaal, H.; Suhm, M. A. **2001**, *99*, 413–425. (b) Yonker, C. R.; Wallen, S. L.; Palmer, B. J.; Garrett, B. C. *J. Phys. Chem.* **1997**, *101*, 9564–9570.
 (53) Ciprani, P.; Nardone, M.; Ricci, F. P.; Ricci, M. A. *Mol. Phys.* **2001**, *99*, 301–308.
 (54) Kauffman, J. F. *J. Phys. Chem. A* **2001**, *105*, 3433–3442.

Table 2. Geometric Parameters of the CO₂ Complexes Formed with HCHO, AcH, MeOAc, AcOH, and DMSO for Different Interaction Configurations, Calculated at the MP2/6-31+G* Level (See Figure 1)^a

molecular species	A ₁ (deg)	A ₂ (deg)	A ₃ (deg)	d (Å)	D (Å)	ΔR (mÅ)	ΔA ₁ (deg)	Δν ₂ (cm ⁻¹)	ΔR _{C-H} (mÅ)	ΔR _{C=O} (mÅ)
HCHO-CO ₂ (T)	178.6	—	—	—	—	0.0	1.4	10.0	-0.10	0.75
HCHO-CO ₂ (P)	178.1	111.0	109.5	2.71	3.24	3.50	1.9	18.0	-0.66	2.06
AcH-CO ₂ (M)	178.1	131.1	143.3	2.66	3.59	3.14	1.9	16.0	-0.39	1.32
AcH-CO ₂ (P)	177.7	112.2	110.6	2.79	3.26	3.48	2.3	22.0	-1.32	1.79
MeOAc-CO ₂ (M)	177.9	132.0	142.6	2.66	3.58	2.73	2.1	18.6	-0.14	2.07
MeOAc-CO ₂ (E)	178.1	157.9	103.0	3.05	3.47	2.50	1.9	9.0	-0.39	1.60
			112.0	2.91					-0.66	
AcOH-CO ₂ (M)	178.0	131.3	144.5	2.57	3.51	4.19	2.0	16.0	-0.12	0.75
DMSO-CO ₂	177.0	—	128.0	2.74	3.52	3.45	3.0	30.0	-0.34	—

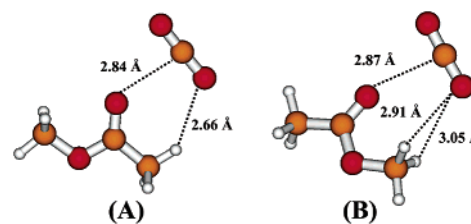
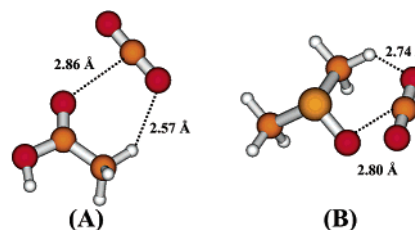
^a The following abbreviations are used: ΔR = R₂ - R₁; ΔR_{C=O} is the change in the carbonyl bond length; ΔA₁ refers to the bending angle of CO₂ (180 - A₁, in degrees).

**Figure 3.** Optimized structures (MP2/6-31+G*) for (A) the methyl side and (B) the proton side interaction geometries of the AcH-CO₂ complex.

other LB (carbonyl and sulfonyl) systems with differences in the LB electron density and other changing structural features. The optimized geometries for the complexes of CO₂ with AcH, MeOAc, AcOH, and DMSO in different interaction geometries are given in Figures 3, 4, and 5 A and B, respectively.

The ΔE^c values at the Hartree-Fock (HF) and MP2 levels using the aug-cc-pVDZ basis set are shown in Table 1. The strongest interaction observed is for the DMSO-CO₂ complex; however, we will discuss DMSO separately and restrict the primary part of the discussion to carbonyl compounds. For AcH (Figure 3, A and B), the T-interaction is energetically unstable, and two different slanted configurations are observed. In the first case, the CO₂ molecule is interacting with acetaldehyde from the methyl side (AcH-CO₂ (M)), and in the other geometry, on the side of the aldehyde proton (AcH-CO₂ (P)). Similarly, for MeOAc, there are two possible interaction geometries, namely, the methyl side (MeOAc-CO₂ (M)) and the ester side (MeOAc-CO₂ (E)) approaches, which are shown in Figure 4, A and B, respectively. For AcOH, only the methyl side configuration (AcOH-CO₂ (M)) was optimized. We did not observe a minimum on the acid side, despite the acid side being less sterically hindered. It is seen from Table 1 that the interaction energies of the CO₂ complexes at the MP2 level are in the order: DMSO < MeOAc (methyl side) < AcOH (methyl side) < AcH (proton side) < MeOAc (ester side) < AcH (methyl side) < HCHO (proton side) < HCHO (T), indicating the strongest interaction for DMSO and the weakest for HCHO (T). All these energies compared to that of HCHO (T) structure support the existence of a cooperative C-H...O interaction in the complexes studied that could lead to enhanced solvation of materials functionalized with these moieties in liquid and scCO₂.

The geometrical parameters for the various complexes are presented in Table 2. For AcH (Figure 3), the >C=O...C angles (A₂) are 131.1° and 112.2° for the methyl side and proton side approaches, respectively. For the methyl side approach, one of the hydrogen atoms of the methyl group (that is planar to the carbonyl group), the methyl carbon, aldehyde carbon, and the CO₂ molecule are coplanar with the carbonyl oxygen interacting

**Figure 4.** Optimized structures (MP2/6-31+G*) for (A) the methyl side and (B) the ester side interaction geometries for the MeOAc-CO₂ complex.**Figure 5.** Optimized structures (MP2/6-31+G*) for (A) the methyl side configuration of the AcOH-CO₂ complex and (B) the DMSO-CO₂ complex.

with the carbon atom of CO₂. The carbonyl oxygen of AcH is a better electron donor compared to that of HCHO due to the electron-donating ability of the methyl group (considering the hyperconjugation with the methyl hydrogen atoms), and this explains the higher ΔE^c for the AcH-CO₂ complexes compared to that of HCHO. The ΔE^c values for the methyl and ester side complexes of MeOAc (Figure 4, A and B) are -2.82 and -2.64 kcal/mol, respectively, and the corresponding >C=O...C angles (A₂) are 132.0° and 157.9°. The methyl side complex of AcOH (Figure 5A) has a ΔE^c of -2.80 kcal/mol and A₂ = 131.3°. All of the above results provide strong evidence for the presence of weak C-H...O interactions, as postulated in Figure 1. Additionally, examination of the geometries of the complexes suggests that these two interactions (LA-LB and C-H...O) act cooperatively. The interaction of the carbonyl group with CO₂ introduces a partial electron density transfer to the carbon atom of the CO₂ molecule while the C-H...O hydrogen bond transfers some electron density back to the carbonyl carbon. Each of these interactions reinforces the other, resulting in a very weak electron delocalization in the five (or six)-membered ring formed by the carbonyl carbon, carbonyl oxygen, the carbon atom of the CO₂, one of the oxygen atoms of the CO₂ (involved in the C-H...O hydrogen bond), and the hydrogen atom attached to the carbonyl group (the methyl proton in the case of the methyl side approaches) as seen in Figures 2-5.

3.2. Contraction of the C–H Bond. It is well established that the C–H bond will undergo shortening as a result of C–H···O hydrogen bonding.^{28–30} Also, assuming an electrostatic model, as for conventional O–H···O hydrogen bonds, the C–H···O hydrogen bonds should ideally be linear, with the hydrogen atom interacting with the lone pair of the oxygen while the C–H bond and the CO₂ unit are coplanar. In the case of normal hydrogen bonds, the directionality of the bond is generally considered as evidence for the existence of the hydrogen bond. However, crystal structure data reveal large deviations, with C–H···O bond angles ranging from 90° to 180°, indicating no preference for linearity.¹⁹ It can also be seen that even in the case of the HCHO–CO₂ (T) complex, where there is no possibility of a C–H···O interaction, we observe a contraction of the aldehydic C–H bond, although this is only 15% of that in the case of the proton side approach involving the cooperative C–H···O interaction. This can be attributed to the increased electron withdrawal by the carbonyl oxygen from the carbonyl carbon as a result of its electron donation to the carbon atom of the CO₂ molecule. From this, it must be concluded that the contraction of C–H bonds occurs when there is either a *through bond* or *through space* electron withdrawal from the C–H bond, and the behavior is a general attribute of the C–H bonds examined. It is observed that in all of the present complexes, there is a contraction in the C–H bond length as a result of the CO₂ interaction (Table 2).

This poses an interesting question regarding the observed C–H bond contraction in the present complexes as to whether this phenomenon is due to an increased electron withdrawal by the carbonyl oxygen, resulting from the complex formation with CO₂ or from C–H···O interaction. The best way to address this question is through the examination of the relative variation of the C–H and C=O bond lengths upon complex formation, although in a cooperative interaction this may be more complicated. Normally, one would expect that if the C–H bond contraction is only attributed to an increased electron withdrawal by the carbonyl oxygen, then the contraction of the C–H bond and the stretching of the C=O bond should be correlated. However, data from Table 2 reveal that this is not the case and suggest a cooperative pair of interactions. For example, in the proton side complexation of HCHO, the ΔR_{C-H} and $\Delta R_{C=O}$ are respectively -0.66 and 2.06 mÅ, while for the proton side complexation of AcH, the ΔR_{C-H} and $\Delta R_{C=O}$ are -1.32 and 1.79 mÅ respectively. This reveals that although these values collectively indicate the strength of the C–H···O interaction, it is difficult to individually consider them as a marker for the strength of the interaction especially in cases such as methyl acetate, where the electron withdrawal is not localized to a single C–H bond.

3.3. Effect of the C–H···O Interaction on CO₂. In all the complexes studied, the CO₂ molecule undergoes bending from its otherwise linear geometry (Table 2) as a result of possible deviation from the sp²-hybridization of the carbon atom upon LA–LB complexation. Aside from this, we noticed another important geometric aspect that supports the presence of the C–H···O interaction. Assuming that the only type of interaction between these carbonyl compounds and CO₂ is the LA–LB interaction, one would expect that the two C=O bond lengths of CO₂ should be identical. Table 2 shows that these distances are not equal except in the case of the HCHO–CO₂ (T)

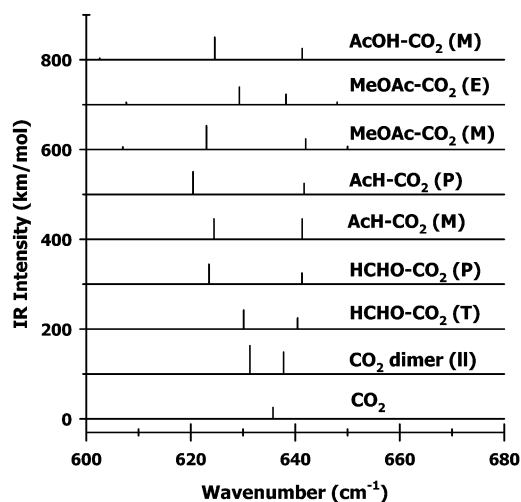


Figure 6. Calculated harmonic IR spectra (MP2/6-31+G*) of the bending mode of CO₂ in CO₂ monomer, CO₂ dimer, HCHO–CO₂ (T), HCHO–CO₂ (P), AcH–CO₂ (M), AcH–CO₂ (P), MeOAc–CO₂ (M), MeOAc–CO₂ (E), and AcOH–CO₂ (M).

complex. In all other systems, the C=O bond that is presumed to be involved in a C–H···O interaction is longer than the “free” C=O bond. This provides strong evidence for the weak C–H···O interaction, but also, one should be able to draw a qualitative correlation between the ΔR (the difference between the two C=O bond lengths of CO₂) and the strength of the C–H···O hydrogen bonding. Accordingly, it can be seen from Table 2 that the strongest C–H···O interaction is in the case of AcOH and decreases in the order AcOH–CO₂ (M) > HCHO–CO₂ (P) > AcH–CO₂ (P) > DMSO–CO₂ > AcH–CO₂ (M) > MeOAc–CO₂ (M) > MeOAc–CO₂ (E). While the O···H distance (d in Figure 1) also could be a measure of the interaction strength, we cannot draw a direct correlation between d and the C–H···O interaction energy since the C–H···O angles are different in these systems and this will also affect the strength of the interaction. Due to the cooperativity, there appears to be an inherent limitation on isolating the energetics of the C–H···O interaction from the LA–LB interaction. This mechanism for the stabilization of the solvation complexes is noteworthy; however, one needs to analyze the intermolecular charge transfer variation in the individual atomic charges upon complex formation, vibrational frequencies, and the changes in the bond lengths to characterize the fundamental nature and extent of these interactions.

3.4. Vibrational Spectra. The calculated harmonic infrared frequencies for the CO₂ bending mode, ν_2 , in the various complexes are shown in Figure 6. It can be seen that the degeneracy of the ν_2 modes of complexed CO₂ is lifted and the values of the vibrational energy separation between these bands, $\Delta\nu_2$, are given in Table 2. For the complex, the in-plane bending mode (with reference to the plane of the interacting Lewis base group and the adjacent carbon atom) is at a lower frequency compared to the out-of-plane mode. The largest splitting is for the DMSO–CO₂ complex (30 cm⁻¹). It is also observed that the in-plane bending mode is more sensitive to the binding and the typical shifts are to lower frequencies. However, the splitting of the ν_2 mode is affected by both the LA–LB as well as the C–H···O interaction, and the individual contributions will change, depending on the specific compounds and the interaction configuration.

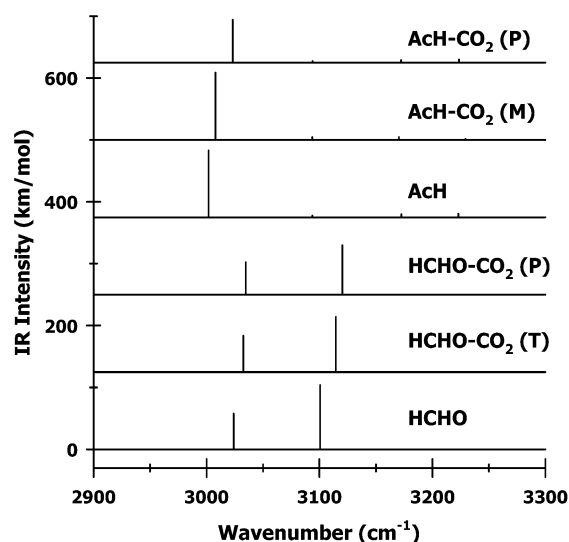


Figure 7. Calculated harmonic IR spectra (MP2/6-31+G*) of the C–H stretching modes in HCHO, HCHO–CO₂ (T), HCHO–CO₂ (P), AcH, AcH–CO₂ (M), and AcH–CO₂ (P).

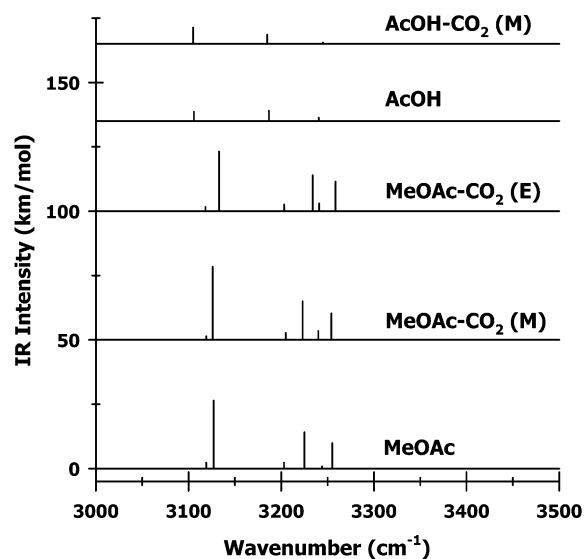


Figure 8. Calculated harmonic IR spectra (MP2/6-31+G*) of the C–H stretching modes in MeOAc, MeOAc–CO₂ (M), MeOAc–CO₂ (E), AcOH, and AcOH–CO₂ (M).

The calculated infrared spectra of the C–H stretching region for the various CO₂ complexes are shown in Figures 7 and 8. As discussed previously, the C–H bonds of the aldehyde groups (or the ^αC–H) undergo contraction, and the IR frequencies are blue-shifted as a result of the increase in energy separation between the excited and ground vibrational states of the complex compared to the monomer. It can be seen from Figure 7 that for HCHO, the C–H stretching mode blue-shifts in both the T geometry and the proton side approach configurations. Also, Figure 7 shows that in the AcH–CO₂ complex, the aldehyde C–H stretching mode blue-shifts in configurations where CO₂ approaches from either the methyl or the proton side. However, for the methyl side interaction, the antisymmetric stretch is slightly blue-shifted, and this is absent for the proton side approach. The trends in the vibrational spectra of the C–H stretching region for MeOAc and AcOH are shown in Figure 8. The blue-shifts of the C–H modes are more pronounced for the ester side interaction, indicating stronger C–H···O interac-

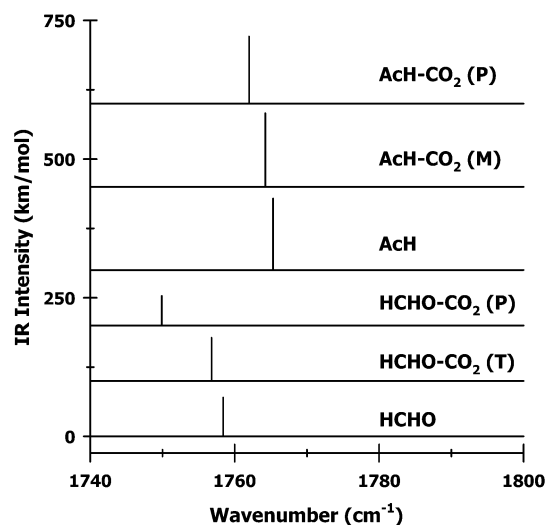


Figure 9. Calculated harmonic IR spectra (MP2/6-31+G*) of the carbonyl stretching modes in HCHO, HCHO–CO₂ (T), HCHO–CO₂ (P), AcH, AcH–CO₂ (M), and AcH–CO₂ (P).

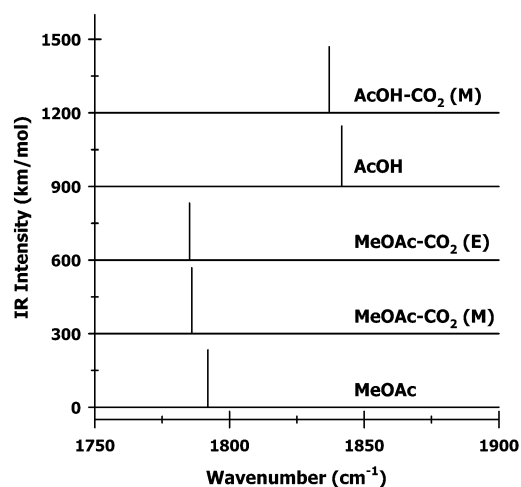


Figure 10. Calculated harmonic IR spectra (MP2/6-31+G*) of the carbonyl stretching modes in MeOAc, MeOAc–CO₂ (M), MeOAc–CO₂ (E), AcOH, and AcOH–CO₂ (M).

tions for the ester side approach. This can be corroborated by the larger contraction of the C–H bonds for the ester side approach. This definitely cannot be attributed to an increased LA–LB interaction since A_2 is 158°, unsuitable for the ideal >C=O···C interaction especially when one considers the steric repulsion. The lower value of $\Delta R_{C=O}$ for the ester side approach (1.6 mÅ) in comparison with that for the methyl side (2.07 mÅ) also supports the hypothesis that there is a C–H···O hydrogen bond in this system.

In a situation where both the C–H···O interaction and the LA–LB interaction are operative, and where both these give rise to the same effects as in the majority of the cases here, the spectral deconvolution that would allow one to attribute the observations to a particular interaction is rather difficult. For a comparison, the carbonyl stretching region of the calculated harmonic infrared frequencies for the different complexes are shown in Figures 9 and 10.

In all the complexes, there is a red-shift in the carbonyl stretching frequency. This is more pronounced for HCHO in the proton side approach of CO₂, although the trend is similar

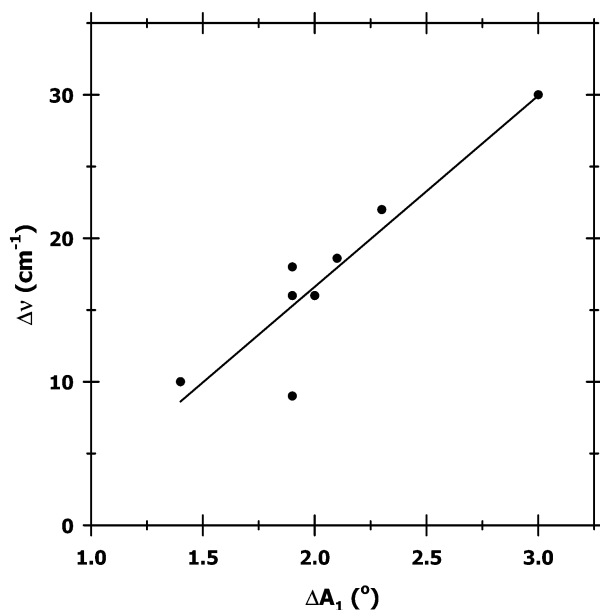


Figure 11. The vibrational energy splitting of the CO₂ bending modes ($\Delta\nu_2$) plotted versus the deviation from linearity (degree of bending for the CO₂ molecule, ΔA_1). The straight line is indicative of the cooperativity of the LA-LB and the C-H...O hydrogen bond interactions (Table 2).

Table 3. Charge Transfer (CT) from the Carbonyl Compound to CO₂ in Millielectrons (me) and the Difference (Δq) between the Charges on the "Free" and "Complexed" Oxygen Atoms of CO₂ for the Various Interaction Complexes

species	charge transfer, CT (me)	Δq (me)
HCHO-CO ₂ (T)	4.9	0.2
HCHO-CO ₂ (P)	10.9	43.6
AcH-CO ₂ (M)	7.9	34.0
AcH-CO ₂ (P)	20.1	33.8
MeOAc-CO ₂ (M)	2.6	27.6
MeOAc-CO ₂ (E)	2.2	22.6
AcOH-CO ₂ (M)	2.8	47.6

for the AcH complexes. For both MeOAc and AcOH, there is a significant red-shift in the carbonyl stretching frequency.

The cooperativity of the LA-LB interaction and the C-H...O interaction should be reflected in the correlation of the splitting of the degenerate ν_2 vibrational modes and the bending of the CO₂ molecule (deviation from linearity) upon complex formation, since these are two parameters that are affected collectively by both interactions. A plot of $\Delta\nu_2$ versus ΔA_1 for the various complexes is given in Figure 11 and is found to be linear, suggesting their common origin. This also supports the cooperativity of the two interactions and the complex manner in which they are mixed.

3.5. Charge-Transfer Model. To gain a clearer view of the C-H...O hydrogen bond and its cooperativity with the LA-LB interaction, we investigated the overall charge transfer (CT) between the LA and LB units involved in the interaction, as well as the changes in the natural population of charges for the atoms involved in complex formation. The charge transferred from the Lewis base unit to CO₂ in various complexes (expressed in millielectrons, me) is given in Table 3.

It is calculated by summing up the atomic charges on either of the individual molecules. The sum of these charges on the isolated monomers should be zero; therefore, the magnitude and sign of the sum of these charges in the complex provide an estimate of the charge transferred from one molecule to the other

Table 4. Change in the Natural Population Atomic Charge (Δq) of Atoms in the Complexes Relative to Monomers for the Atoms Involved in the C-H...O and the $>C=O...C$ Interactions (Δq_H for Water Dimer³⁰ Is 19 me)

species	C-H...O			$>C=O...C_2$		
	Δq_C (me)	Δq_H (me)	Δq_O (me)	$\Delta q_{C(1)}$ (me)	Δq_O (me)	$\Delta q_{C(2)}$ (me)
HCHO-CO ₂ (T)	3.87	3.5	1.0	3.9	-5.8	-3.2
HCHO-CO ₂ (P)	-1.1	19.3	-27.0	-1.1	-21.5	-0.4
AcH-CO ₂ (M)	-4.2	18.5	-17.6	6.35	-22.7	-6.8
AcH-CO ₂ (P)	166.8	22.5	-19.8	166.8	-25.3	26.0
MeOAc-CO ₂ (M)	-47.5	26.9	-15.6	52.7	-50.9	0.1
MeOAc-CO ₂ (E)	-14.6	0.0, 8.2	-15.6	38.3	-30.8	-0.6
AcOH-CO ₂ (M)	-24.7	20.3	-26.6	40.7	-51.2	2.7

as a result of the complex formation. From Table 3, it is seen that the charge transfer is most pronounced in the proton side configurations for AcH (20.1 me) and HCHO (10.9 me).

Another interesting parameter to compare in these complexes would be the relative charges on the two oxygen atoms of CO₂, as the degeneracy of these oxygen atoms is lifted on complex formation, presumably as a result of C-H...O hydrogen bonding. The differences between the Mulliken charges on these two oxygen atoms of CO₂ are also shown in Table 3. For the CO₂ molecule, in all cases the "complexed" oxygen atom involved in the C-H...O hydrogen bond is more negative compared to the "free" oxygen, making it more attractive toward the bridging hydrogen. It is noteworthy that while there is almost no difference between the two oxygen atoms of CO₂ for the T-geometry of HCHO-CO₂, there is clearly a large difference in the proton side configuration of HCHO-CO₂, providing further evidence for the existence of the C-H...O interaction. These are also well correlated with the differences between the bond lengths of the two C=O bonds of CO₂ in these complexes (ΔR), except for the small deviation in the case of AcH.

An examination of the changes in the natural population atomic charges for the various atoms involved in the LA-LB ($>C=O...C$) and the C-H...O interactions should reflect the electron density shifts, and these are presented in Table 4. Negative charges indicate a net gain in electron density, while positive charges indicate a net loss of electron density. For the LA-LB interaction ($>C=O...C$ triad), the carbonyl oxygen in all the complexes shows a net gain in electron density as expected due to an increased polarization of the carbonyl group, while the carbonyl carbon has a loss of electron density (with the exception of HCHO-CO₂ (P), where the carbonyl carbon acquires a small negative charge, -1.1 me). The carbon atom of the CO₂ molecule has an even reversal of electron density changes, but strikingly, the AcH-CO₂ (P) complex shows a high net positive charge (26.0 me), indicating loss of electron density, despite the transfer of electron density from the carbonyl group to CO₂ (LA-LB interaction). This loss of electron density in the carbon atom of CO₂ may be attributed to the increased polarization of one of the C=O bonds of CO₂ as a result of its involvement in the C-H...O hydrogen bonding.

For the C-H...O triad, it is shown in Table 4 that, while the oxygen atom of CO₂, as well as the carbon atom acquire a net negative charge in all complexes with the exception of AcH-CO₂ (P), the bridging hydrogen acquires a net positive charge. For the AcH-CO₂ (P) complex, both the carbon and hydrogen of the C-H...O triad loses electron density, while the oxygen atom gains electron density as in the other systems. The general

trend is consistent with that observed for conventional hydrogen bonds, as observed in a H₂O dimer. The observed gain of positive charge on the bridging hydrogen atom is higher in comparison with that of the water dimer. This larger increase in the positive charge of the bridging hydrogen, however, will make this hydrogen more attractive to the negatively charged oxygen atom of the CO₂ molecule, enhancing the strength of the C–H···O bond. The observed gain in the electron density of the carbon atom of the C–H···O triad, despite the increased electron withdrawal by the carbonyl group as a result of the LA–LB interaction, also supports the formation of the C–H···O bond.

The pattern of the charge density changes on these CO₂ complexes, in any case, provides conclusive evidence for the existence of a C–H···O hydrogen bond as an additional stabilization mechanism for the LA–LB complexes between carbonyl groups and CO₂ in the systems studied. Also, the cooperative nature of these two interactions can be examined from a different point of view on the basis of the net changes in the atomic charges on the individual atoms involved. For example, the C–H···O interactions make the oxygen atom of CO₂ more electron-rich, most likely at the cost of the carbon atom of CO₂, making it more positive. This in turn, enhances the strength of its LA–LB interaction with the carbonyl group.

3.6. DMSO–CO₂ Interactions. For DMSO, the optimized geometry is somewhat different compared to that of the carbonyl compounds. In this case, unlike in the carbonyl systems, the S–O–C–O dihedral is nonzero (Figure 5B). A qualitative explanation for this would be that while in the carbonyl systems the oxygen is purely sp²-hybridized making the lone pairs of oxygen in plane, the oxygen of the sulfonyl oxygen is intermediate between the sp² and sp³ hybridizations due to the highly polarized S=O bond. This also results in a stronger LA–LB interaction. We also observe a contraction of –0.34 mÅ for the C–H bond involved in the C–H···O hydrogen bonding. Maximum bending of CO₂ (3°) is observed in this complex, as well as the highest splitting of the ν₂ bending modes of CO₂ indicating that both the LA–LB and the C–H···O interaction are significant for DMSO. All these suggest that in the case of sulfonyl moieties too, αC–H bonds can enhance the strength of the CO₂-philic interactions through cooperative C–H···O interactions.

3.7. Role of the C–H···O Interaction on Solvation. As mentioned at the beginning of the discussion, solvation in liquid and scCO₂ depends on the relative strengths of solvent–solvent, solute–solvent, and solute–solute interactions apart from entropic considerations. While the interaction energy of the CO₂ dimer alone cannot represent exactly the solvent–solvent interaction cross-section in liquid and scCO₂ due to the presence of many-body interactions, it provides a starting point for estimating the strength of solvent–solvent interactions. The results of the calculations in this work show that for all the simple carbonyl systems studied, the solute–solvent interaction is significantly stronger than the solvent–solvent interaction. This favors solvation of these materials in liquid and scCO₂, suggesting that hydrocarbons functionalized with these carbonyl moieties may exhibit good CO₂-philicity. However, the solvation also depends strongly on the lattice energies of the CO₂-philes that are functionalized with these carbonyl moieties. We do not have sufficient experimental data available to determine which

functionality is better as far as lattice energy requirements are concerned. Additionally, one needs to consider how cooperative solute–solvent C–H···O interactions may enhance the solubility of materials in liquid and scCO₂, since in most of these materials a significant portion of the lattice energy comes from C–H···O interactions. For example, it was suggested recently that the C–H···O hydrogen bonds are responsible for the self- and cross-associations of cyclic and linear carbonates, resulting in significant differences in many physical properties.⁵⁵ Since the cooperative C–H···O hydrogen bonds increase the effective solute–solvent interactions, they definitely will contribute to the enhanced solvation of materials in liquid and scCO₂.

Following our calculations, we identified acetate groups as the most favored CO₂-philic functional group based on the carbonyl functionality. Since nature is abundant with polyhydroxy compounds in the form of carbohydrates, we expected that the acetylation of carbohydrates would be a previously unknown resource of renewable CO₂-philes. In fact, we have recently reported that acetylated sugars undergo deliquescence in gaseous CO₂ and exhibit an extremely high solubility in scCO₂ (above 30 wt %) at very low pressures.⁵⁶ Crystal structures of sugar acetates also reveal that the intermolecular C–H···O interactions between the carbonyl group of the acetate moiety and αC–H bonds provide the most stabilizing interactions in the lattice. From these observations and the present calculations, we propose that the cooperative C–H···O interaction plays a unique role in enhancing solubility of these materials in scCO₂. The function of these interactions in the solvation of polycarbonyl compounds in liquid and scCO₂ may be important not only in terms of the specific solute–solvent interaction but also in terms of replacing the C–H···O interactions in the lattice by the “CO₂-philic” C–H···O interactions upon solvation.

4. Conclusions

The role of a cooperative C–H···O interaction as an additional stabilizing interaction along with the LA–LB interaction between CO₂ and carbonyl compounds with hydrogen atoms attached to the carbonyl carbon or the α-carbon atom and their implications for solvation in scCO₂ are investigated in this work. Ab initio calculations are performed on complexes of CO₂ with model carbonyl systems such as HCHO, AcH, MeOAc, and AcOH. Calculations are also performed on the CO₂–DMSO complex to investigate the possible use of the sulfonyl moiety as a CO₂-philic functional group. The calculations reveal that among the carbonyl systems investigated, MeOAc has the strongest interaction with CO₂. The high CO₂-philicity of MeOAc suggests that acetylation, unlike fluorination, could be a much cheaper method for the design of renewable CO₂-philes. Considering the abundance of polyhydroxy compounds in nature, this method offers great possibilities toward enabling sustainable, green chemistry applications in CO₂-based solvent systems. The results also suggest that incorporation of S=O bonds could be an effective approach to the design of CO₂-philic materials and explain the high miscibility of DMSO in CO₂.

In all cases the bond electron density of CO₂ is more polarized toward the oxygen atoms, leaving a partial positive charge on the carbon atom and negative charge on the oxygen atoms. This

(55) Wang, Y.; Balbuena, P. B. *J. Phys. Chem. A* **2001**, *105*, 9972–9982.

(56) Raveendran, P.; Wallen, S. L. *J. Am. Chem. Soc.* **2002**, *124*, 7274–7275.

makes the carbon atom an electron acceptor in a Lewis acid–Lewis base interaction with carbonyl groups, which act as Lewis bases. Also, the oxygen atoms having partial negative charges can be involved in weak electrostatic interactions with properly placed electron-deficient C–H bonds. In all the complexes studied, the CO₂ molecule is bent from its otherwise linear geometry as a result of this interaction. The two C=O bonds of the “complexed” CO₂ are nonidentical. The C=O bond involved in the C–H···O interaction is consistently longer than the “free” C=O, strongly supporting the presence of these interactions. Charge transfer and electron density changes in the systems upon complexation also provide conclusive evidence for the existence of the C–H···O hydrogen bond. The question remains as to the relative contribution of the C–H···O interaction to the overall stabilization, but such an estimate is elusive at present, considering the intricate nature of the cooperativity

of these interactions. The investigations, nevertheless, reveal the presence of a previously unreported, cooperative C–H···O hydrogen bond that merits consideration when designing CO₂-philic materials. The generality of these results with respect to designing cooperative interactions into synthetic schemes for enhanced solubility in CO₂ is a topic for future investigation.

Acknowledgment. The material presented here is based on work supported in part by the University of North Carolina, Department of Chemistry, through start-up funds, the STC Program of the National Science Foundation under Agreement No. CHE-9876674, and by Merck & Co., Inc. We also thank the North Carolina Supercomputing Center for computational resources, Dr. Lalith Perera for computational assistance and the members of our research group for helpful discussions.

JA0174635